Structural Analysis of Cylindrical and Spherical Supramolecular Dendrimers Quantifies the Concept of Monodendron Shape Control by Generation Number

V. Percec,*,† W.-D. Cho,† P. E. Mosier,† G. Ungar,‡ and D. J. P. Yeardley‡

Contribution from The W. M. Keck Laboratories for Organic Synthesis, Department of Macromolecular Science, Case Western Reserve University, Cleveland, Ohio 44106-7202, and Department of Engineering Materials and Center for Molecular Materials, University of Sheffield, Sheffield S1 3JD, U.K.

Received June 1, 1998

Abstract: In 1989, it was predicted that a change in dendritic shape to a nearly spherical one should occur upon increasing the generation number (Naylor, A. M.; Goddard, W. A., III; Kiefer, G. E.; Tomalia, D. A. *J. Am. Chem. Soc.* **1989**, *111*, 2339). The absence of long-range order required for X-ray analysis allowed only indirect evidence to be provided for this concept. This publication reports the synthesis of three generations of self-assembling monodendrons based on the AB_3 building block methyl 3,4,5-trihydroxybenzoate. The first 3,4,5-tris[*p*-(*n*-dodecan-1-yloxy)benzyloxy]benzoic acid and the second-generation methyl 3,4,5-tris{3′,4′,5′-tris[*p*-(*n*-dodecan-1-yloxy)benzyloxy]benzyloxy}benzoate monodendrons self-assemble into cylindrical supramolecular dendrimers that self-organize in a two-dimensional p6mm lattice. The third-generation monodendron 3,4,5-tris(3′,4′,5′-tris{3″,4″,5″-tris[*p*-(*n*-dodecan-1-yloxy)benzyloxy]benzyloxy}benzyloxy)-benzoate self-assembles in a spherical dendrimer that self-organizes in a three-dimensional cubic $Pm\bar{3}n$ lattice. Structural analysis of these lattices by X-ray diffraction provided the first direct demonstration of the supramolecular dendrimer shape change from cylindrical to spherical and indirect determination of the average shape change of the monodendron from a quarter of a disk to a half of a disk and to a sixth of a sphere as a function of generation number. These results have demonstrated the concept of monodendron and supramolecular dendrimer shape control by generation number.

Introduction

Molecular and supramolecular monodendrons and dendrimers provide some of the most powerful synthetic building blocks available today for the construction of giant macromolecular and supramolecular systems with complex architecture and precise shape and functionality.[1] Rational design and construction of these building blocks requires the elaboration of dendrons of well-defined shape. *A seminal paper*[2] *published in 1989 predicted, by a combination of molecular modeling and theoretical calculations, that a change in dendritic shape should occur upon increasing the generation number. The dendrimers used in these experiments did not self-organize on a lattice with the long-range order needed for X-ray investigations; therefore, no detailed experimental structural data were available at that time to quantitatively and definitively demonstrate the concept of molecular shape control by generation number.* A discontinuity frequently observed in the dependence of various physical parameters of dendrimers and monodendrons as a function of generation number, sometimes referred to as *the dendrimer effect*, has been used to indirectly indicate a structural change to a spherical shape. Changes in the hydrodynamic volume,[3a,b] intrinsic viscosity, hydrodynamic radii and refraction index increment,[3c] dipole moment,[3d] and various photophysical parameters[1g,3e−h] have been used to estimate that a shape change occurs at the third-, fourth-, or fifth-generation in solution. A change in the melt viscosity of dendrimers was associated with their shape change in the melt state.[4] This indirect evidence has been only recently accompanied by more quantitative experiments on shape in melt by a combination of site-specific

† Case Western Reserve University.

‡ University of Sheffield.

(1) (a) Tomalia, D. A.; Esfand, R. *Chem. Ind.* **1997**, 416. (b) Tomalia, D. A.; Naylor, A. M.; Goddard, W. A., III. *Angew. Chem., Int. Ed. Engl.* **1990**, *29*, 138. (c) Fréchet, J. M. J. *Science* **1994**, *263*, 1710. (d) Fréchet, J. M. J.; Hawker, C. J. In *Comprehensive Polymer Science*, 2nd Suppl.; Allen, G., Ed.; Elsevier: Oxford, 1996; pp 77−132. (e) Newkome, G. R.; Moorefield, C. N.; Vögtle, F. *Dendritic Molecules. Concepts, Synthesis, Perspectives*; VCH: Weinheim, 1996. (f) Moore, J. S. *Acc. Chem. Res.* **1997**, *30*, 402. (g) Jiang, D. L.; Aida, T. *Nature* **1997**, *388*, 454. (h) van Hest, J. C. M.; Delnoye, D. A. P.; Baars, M. W. P. L.; van Genderen, M. H. P.; Meijer, E. W. *Science* **1995**, *268*, 1592. (i) Knapen, J. W. J.; van der Made, A. W.; de Wilde, J. C.; van Leeuwen, P. W. N. M.; Wijkens, P.; Grove, D. M.; van Koten, G. *Nature* **1994**, *372*, 659. (j) Percec, V.; Chu, P.; Ungar, G.; Zhou, J. *J. Am. Chem. Soc.* **1995**, *117*, 11441. (k) Meier, H.; Lehmann, M. *Angew. Chem., Int. Ed. Engl.* **1998**, *37*, 643. (l) McElhanon, J. R.; McGrath, D. V. *J. Am. Chem. Soc.* **1998**, *120*, 1647.

(2) Naylor, A. M.; Goddard, W. A., III; Kiefer, G. E.; Tomalia, D. A. *J. Am. Chem. Soc.* **1989**, *111*, 2339.

(3) (a) Hawker, C. J.; Fréchet, J. M. J. *J. Am. Chem. Soc.* **1990**, *112*, 7638. (b) Hawker, C. J.; Malmström, E. E.; Frank, C. W.; Kampf, J. P. *J. Am. Chem. Soc.* **1997**, *119*, 903. (c) Mourey, T. H.; Turner, S. R.; Rubinstein, M.; Fréchet, J. M. J.; Hawker, C. J.; Wooley, K. L. *Macromolecules* **1992**, *25*, 2401. (d) Wooley, K. L.; Hawker, C. J.; Fréchet, J. M. J. *J. Am. Chem. Soc.* **1993**, *115*, 11496. (e) Moreno-Bondi, M. C.; Orellana, G.; Turro, N. J.; Tomalia, D. A. *Macromolecules* **1990**, *23*, 912. (f) Caninazi, G.; Turro, N. J.; Tomalia, D. A. *J. Am. Chem. Soc.* **1990**, *112*, 8515. (g) Hawker, C. J.; Wooley, K. L.; Fréchet, J. M. J. *J. Am. Chem. Soc.* **1993**, *115*, 4375. (h) Devadoss, C.; Bharathi, P.; Moore, J. S. *Angew. Chem., Int. Ed. Engl.* **1997**, *36*, 1633.

(4) Hawker, C. J.; Farrington, P. J.; Mackay, M. E.; Wooley, K. L.; Fréchet, J. M. J. *J. Am. Chem. Soc.* **1995**, *117*, 4409.

10.1021/ja9819007 CCC: $15.00
Published on Web 10/16/1998

Scheme 1. Schematic Representation of (a) the Self-Assembly of Flat Tapered Monodendrons into a Supramolecular Cylindrical Dendrimer and the Subsequent Self-Organization of the p6mm Hexagonal Columnar (Φ_h) LC Assembly and (b) the Self-Assembly of Conical Monodendrons into a Supramolecular Spherical Dendrimer and the Subsequent Self-Organization of the $Pm\bar{3}n$ Cubic (Cub) LC Assembly

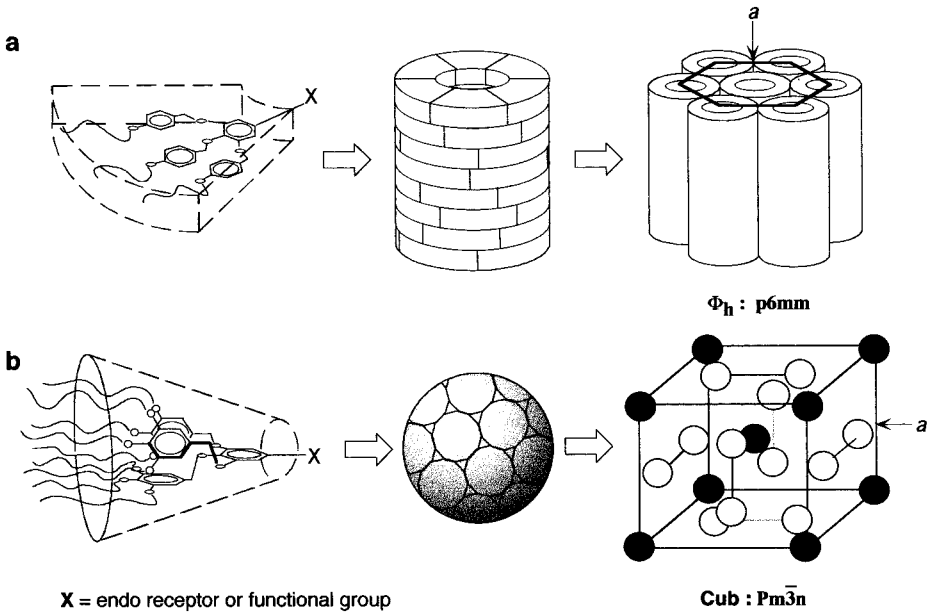

stable-isotope-labeling, rotational-echo double-resonance (REDOR) NMR and distance-constrained molecular dynamic simulations,[5a] and in solution by SAXS.[5b] All these results were generated with AB_2 type dendrimers.

We have recently elaborated a structural analysis method[6−10] that allows the determination of the shape and size of self-assembling monodendritic building blocks[11] by the X-ray analysis of the liquid crystalline (LC) lattice self-organized from their supramolecular dendrimers. In a LC lattice, despite the existence of long-range order (i.e., crystallographic lattice) in density fluctuations, there is no long-range order in the atomic or molecular positions. The reasons for high and low densities are associated respectively with predominantly aromatic and aliphatic regions, both of which are liquidlike.[11] Therefore, this X-ray analysis provides access to the direct determination of the shape of supramolecular dendrimers and to the indirect determination of the shape of their monodendritic building blocks. Presently this method allows the structural analysis of cylindrical[6,8−10] and spherical[7−10] supramolecular and macromolecular dendrimers and permits the determination of the flat tapered, half-disk, conical, and hemispherical shapes of monodendritic building blocks. Scheme 1a outlines the self-assembly of flat tapered monodendrons in a cylindrical supramolecular dendrimer and its subsequent self-organization in a two-dimensional hexagonal columnar p6mm lattice. Scheme 1b shows the self-assembly of conical monodendrons into a spherical supramolecular dendrimer and its subsequent self-organization in a three-dimensional cubic $Pm\bar{3}n$ lattice. Since both the p6mm and $Pm\bar{3}n$ lattices are liquid crystalline rather than crystalline, they generate a thermodynamically controlled self-assembly process. It is well established that the first generation of the AB_3 3,4,5-tris[*p*-(*n*-dodecan-1-yloxy)benzyloxy]benzoic acid monodendron (known as **DOBOB**, or **12-ABG**) self-assembles into a supramolecular cylinder, which self-organizes in a hexagonal columnar lattice.[6,12] Therefore, the first generation of this AB_3 monodendron has a flat tapered shape.[6] Based on theoretical predictions,[2] upon increasing the generation number, the shapes of both the monodendron and the resulting supramolecular dendrimer should change, ultimately reaching a spherical shape.

The goal of this publication is to report the synthesis of three generations of the AB_3-based self-assembling 12-ABG monodendron and describe the first determination of the shape change of both monodendrons and supramolecular dendrimers as a function of generation number. These results will provide a demonstration of the concept of molecular shape control of monodendron and dendrimer via generation number.[2]

Results and Discussion

Synthesis of Monodendrons. The synthesis of 12-ABG benzyl ether monodendrons is outlined in Scheme 2. It follows a convergent approach[13] and a synthetic methodology elaborated previously in our laboratory for the preparation of a related class of monodendrons.[7] The sequence of reactions used in the synthesis of **4** was described previously.[14] Its reduction with $LiAlH_4$ in THF produced **6** in 92.8% yield. The benzyl alcohol group of **6** was chlorinated with $SOCl_2$ of 99.5+% purity in

(5) (a) Wooley, K. L.; Klug, C. A.; Tasaki, K.; Schaefer, J. *J. Am. Chem. Soc.* **1997**, *119*, 53. (b) Kleppinger, R.; Reynaers, H.; Desmedt, K.; Forier, B.; Dehaen, W.; Koch, M.; Verhaert, P. *Macromol. Rapid Commun.* **1998**, *19*, 111.

(6) Percec, V.; Johansson, G.; Ungar, G.; Zhou, J. *J. Am. Chem. Soc.* **1996**, *118*, 9855.

(7) Balagurusamy, V. S. K.; Ungar, G.; Percec, V.; Johansson, G. *J. Am. Chem. Soc.* **1997**, *119*, 1539.

(8) Hudson, S. D.; Jung, H.-T.; Percec, V.; Cho, W.-D.; Johansson, G.; Ungar, G.; Balagurusamy, V. S. K. *Science* **1997**, *278*, 449.

(9) Percec, V.; Ahn, C.-H.; Ungar, G.; Yeardley, D. J. P.; Möller, M.; Sheiko, S. S. *Nature* **1998**, *391*, 161.

(10) Percec, V.; Schlueter, D.; Ungar, G.; Cheng, S. Z. D.; Zhang, A. *Macromolecules* **1998**, *31*, 1745.

(11) (a) de Gennes, P.-G. *Angew. Chem., Int. Ed. Engl.* **1992**, *31*, 842. (b) de Gennes, P.-G.; Prost, J. *The Physics of Liquid Crystals*; Oxford University Press: Oxford, 1993. (c) Percec, V. In *Handbook of Liquid Crystal Research*; Colings, P. J., Patel, J. S., Eds.; Oxford Universtiy Press: Oxford, 1997; pp 259−346.

(12) (a) Malthête, J.; Collet, A.; Levelut, A.-M. *Liq. Cryst.* **1989**, *5*, 123. (b) Malthête, J.; Davidson, P. *Bull. Soc. Chim. Fr.* **1994**, *131*, 812.

(13) Hawker, C. J.; Fréchet, J. M. J. *J. Am. Chem. Soc.* **1990**, *112*, 7638.

Scheme 2. Synthesis of Monodendrons[a]

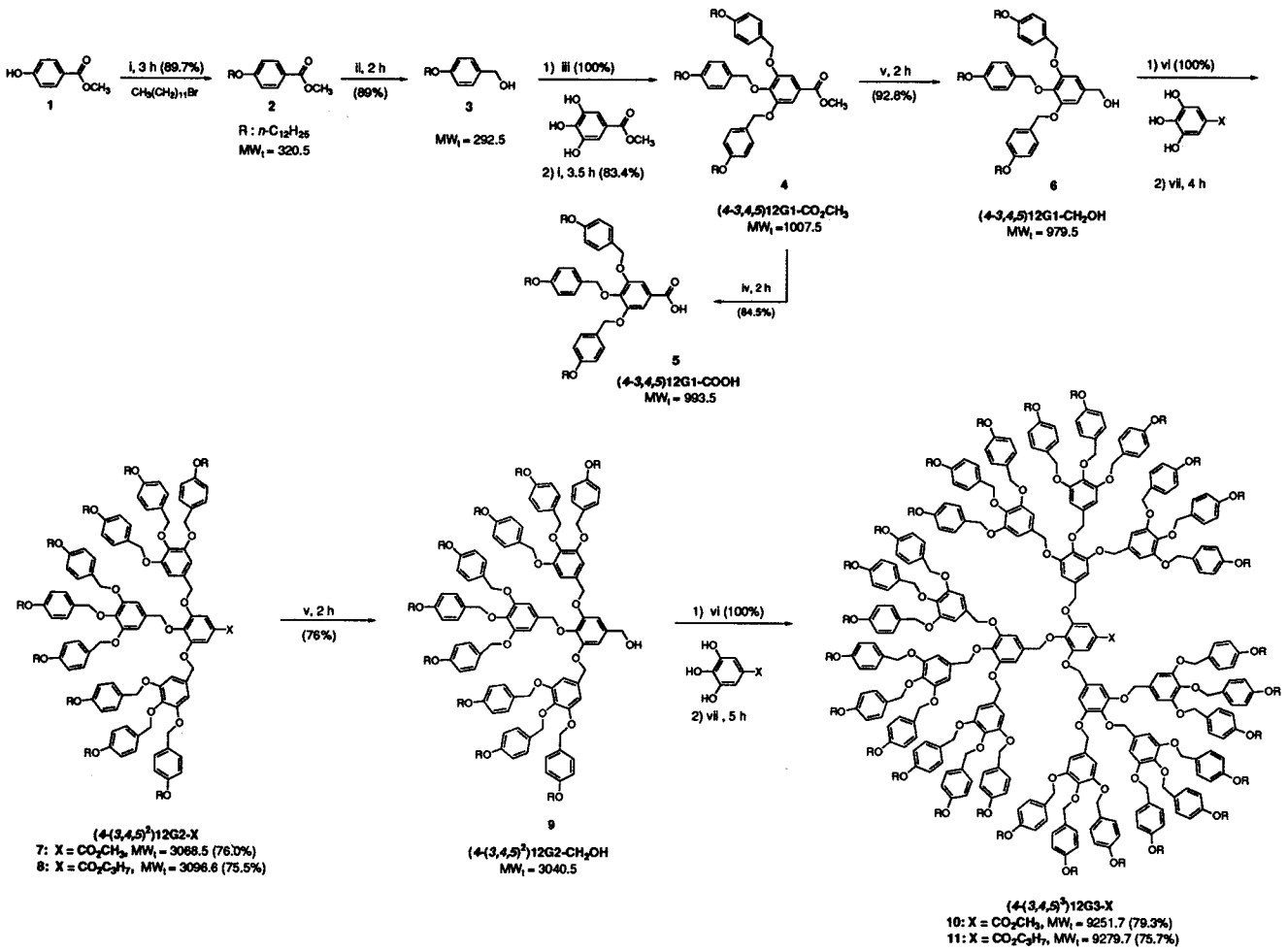

[a] Reagents and conditions: (i) K_2CO_3, DMF, 65 °C; (ii) $LiAlH_4$, Et_2O, 20 °C; (iii) $SOCl_2$, CH_2Cl_2, DMF (cat), 20 °C; (iv) KOH, EtOH, reflux, 50% aqueous CH_3COOH; (v) $LiAlH_4$, THF, 20 °C; (vi) $SOCl_2$, DTBMP, CH_2Cl_2, 20 °C; (vii) K_2CO_3, DMF, THF, 70 °C.

dry CH_2Cl_2 in the presence of 2,6-di-*tert*-butyl-4-methyl pyridine (**DTBMP**)[17] proton trap at 20 °C. The resulting benzyl chloride was used in the next reaction step, without purification, immediately after CH_2Cl_2 was distilled in a rotary evaporator at 20 °C. The use of any other organic base as HCl acceptor and of $SOCl_2$ and CH_2Cl_2 of lower purities cleaves the benzyl ether groups during the chlorination step.[7] Etherification of methyl and propyl gallate with the benzyl chloride of **6** was performed in a mixture of DMF and THF (5:1) at 70 °C in the presence of K_2CO_3 as base to yield **7** in 76% yield and **8** in 75.5% yield. Elimination of O_2 from the reaction mixture is essential during this etherification. Quantitative alkylation occurs in about 4 h. Purification of the resulting compounds is performed by a combination of column chromatography (basic Al_2O_3/CH_2Cl_2) followed by recrystallization from acetone/CH_2Cl_2 (1:3). Reduction of **7** and **8** with $LiAlH_4$ yields **9** in 76% yield. Chlorination of **9** was carried out under reaction conditions similar to those for **6**, and the resulting benzyl chloride was immediately used to alkylate methyl and propyl gallate under conditions similar to those used for the synthesis of **2**, **4**, **7**, and **8**. **10** was obtained in 79.3% and **11** in 75.7% yields. The acid **5** was obtained by the hydrolysis of the parent ester **4** with KOH in a mixture of EtOH and THF (2:3) at reflux followed by neutralization with 50% aqueous CH_3COOH (Scheme 2). A symmetric model for **7** and **8** (i.e., **12**) was synthesized by the alkylation of phloroglucinol (1,3,5-trihydroxybenzene) with the benzyl chloride of **6** (Scheme 3). All compounds were analyzed by a combination of ^1H and ^{13}C NMR spectroscopy, TLC, HPLC, and elemental analysis and were shown to be of purity higher than 99.9%.

Thermal Analysis. The phase behavior of all monodendrons was analyzed by a combination of thermal optical polarized microscopy (TOPM) and differential scanning calorimetry (DSC). Thermal transitions were determined by DSC and the phase behavior was qualitatively assigned by TOMP.[6,7] Cubic mesophases are optically isotropic, while hexagonal columnar mesophases are characterized by a focal conic fan-shaped anisotropic texture (Figure 1). The cubic mesophase corresponds to the $Pm\bar{3}n$ 3-D lattice generated from spherical supramolecular dendrimers, while the hexagonal columnar phase corresponds to the p6mm 2-D lattice generated from cylindrical supramolecular dendrimers. Figure 2 shows representative DSC traces (first heating in a, first cooling in b, and second heating in c) of **4**, **7**, **8**, **10**, and **11**. Transition temperatures, together with their enthalpy changes collected from DSC traces of all

(14) (a) Johansson, G.; Percec, V.; Ungar, G.; Abramic, D. *J. Chem. Soc., Perkin Trans. 1* **1994**, 447. (b) Percec, V.; Johansson, G.; Heck, J.; Ungar, G.; Batty, S. V. *J. Chem. Soc., Perkin Trans. 1* **1993**, 1411. (c) Percec, V.; Heck, J.; Tomazos, D.; Falkenberg, F.; Blackwell, H.; Ungar, G. *J. Chem. Soc., Perkin Trans. 1* **1993**, 2799. (d) Malthête, J,; Tinh, N. H.; Levelut, A. M. *J. Chem. Soc., Chem. Commun.* **1986**, 1548.

(15) Yin, R.; Zhu, Y.; Tomalia, D. A.; Ibuki, H. *J. Am. Chem. Soc.* **1998**, *120*, 2678 and references therein.

(16) Ungar, G.; Abramic, D.; Percec, V.; Heck, J. A. *Liq. Cryst.* **1996**, *21*, 73.

(17) Anderson, A. G.; Stang, P. J. *J. Org. Chem.* **1976**, *41*, 3034.

Scheme 3. Synthesis of **12**[a]

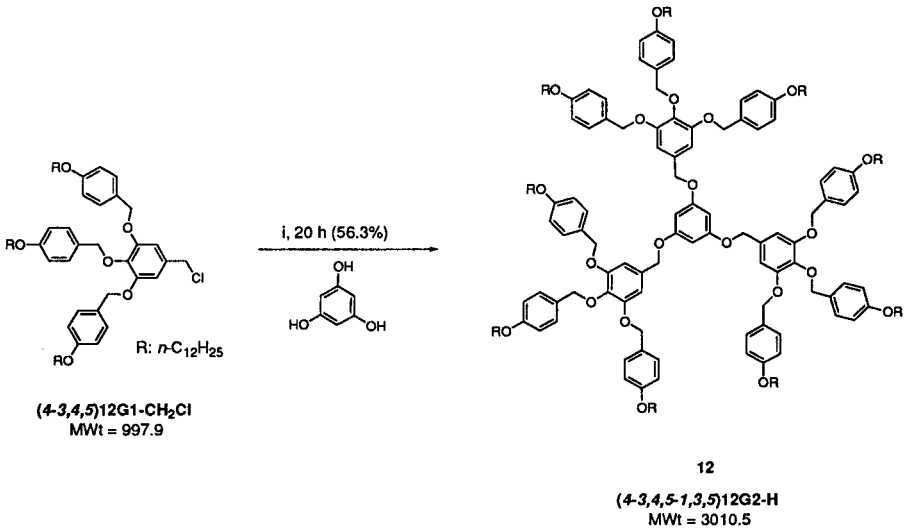

[a] Reagents and conditions: (i) K_2CO_3, DMF, THF, 70 °C.

Figure 1. Representative optical polarized texture exhibited by the hexagonal columnar (Φ_h) mesophase of **8** obtained upon cooling from 97 to 94.4 °C at 1 °C/min.

compounds, are summarized in Table 1. The density at 20 °C for all these compounds is also reported in Table 1. Following this qualitative analysis, selected samples were analyzed by XRD according to the techniques elaborated and described in detail in previous publications.[6,7]

Structural Analysis by XRD. Table 2 summarizes the analysis of the hexagonal columnar and cubic lattices generated from the supramolecular objects self-assembled from **5**, **7**, **8**, **11**, and **12**. The driving force for the self-assembly of related monodendrons was described in previous publications[6−8] and is of no interest for the present discussion. The most significant message generated by Table 2 is as follows. The first two generations of monodendrons self-assemble into cylindrical supramolecular dendrimers. The stratum of the supramolecular cylindrical dendrimers self-assembled from **5** is formed from four monodendrons, while the cylinder self-assembled from **7**, **8**, and **12** is formed from two monodendrons. The third-generation monodendron **11** self-assembles into a spherical supramolecular dendrimer. This spherical dendrimer contains six monodendrons.

Analysis of the Shape of Supramolecular Dendrimers and the Determination of the Average Shape of the Monodendrons. Scheme 4 outlines the self-assembly of the monodendritic building blocks into supramolecular dendrimers and their self-organization in lattices as a function of generation number. There is a continuous change in the shape of the monodendron that is induced by the generation number. The first-generation monodendron has a flat tapered shape equal to a quarter of a disk. The second-generation monodendron has a half of a disk shape. The third-generation monodendron undergoes the most dramatic change in shape and becomes a sixth of a sphere. Since the change from generation two to generation three produces the most dramatic change in the shape of the supramolecular dendrimer resulting from these building blocks i.e., from cylindrical to spherical, we expect that, at this generation number, the physical properties would have to show a discontinuity as the one indirectly detected from evaluation of their physical properties.[1] At this point, we can compare the self-assembly of the third-generation monodendron **10** with that of the similar fourth-generation monodendron, containing 3-alkyl groups on the benzyl ether group, from its periphery reported previously.[7] This comparison is schematically illustrated in Scheme 5. First, we have to mention that the only difference between the fourth-generation monodendron reported previously[7] and the third-generation monodendron **10** is the three alkyl tails on each exterior repeat unit of the fourth-generation compound versus one alkyl tail on each exterior repeat unit of the third-generation compound. The aromatic parts of these two monodendrons are identical. As we can see from Scheme 5, the increase in the number of alkyl tails on the peripheral repeat unit increases the size of the monodendron from a sixth of a sphere to a half of a sphere (i.e., to a hemisphere). We believe that this is a remarkable result that can be exploited in the design of supramolecular monodendritic building blocks with well-defined shape.

A reinspection of Schemes 2 and 3 raises the following question. The structure of monodendrons **7** and **8** can be envisioned to correspond to half of a disk due to their 3,4,5-trisubstitution with **6**. However, the more symmetrically 1,3,5-trisubstituted **12** seems to resemble more a single disklike molecule. The comparative structural analysis of the supramolecular cylindrical dendrimers resulted from these two monodendrons is presented in Table 3. The results from this table show that a single disk generated from **8** or **12** would fit the geometrical and density requirements with a distance between the column strata of 2.58 and 2.56 Å, respectively. These values are below the van der Waals distance of 3.74 Å and are,

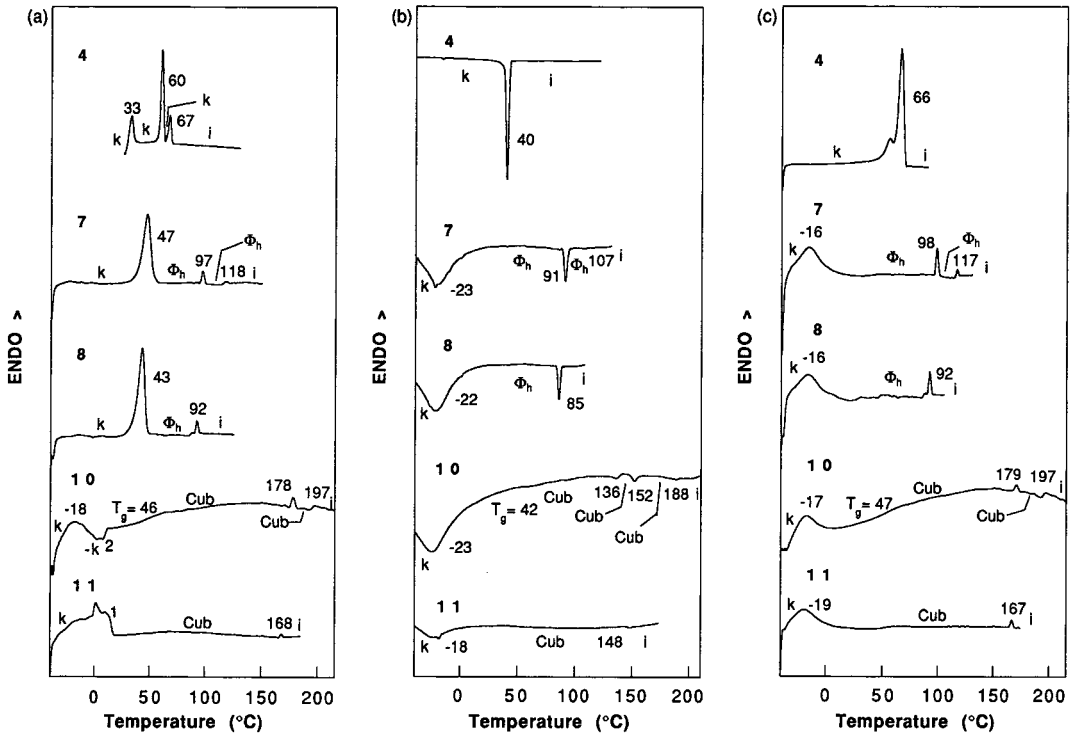

Figure 2. Representative DSC traces (10 °C min^{-1}) of **4**, **7**, **8**, **10**, and **11**: (a) first heating, (b) first cooling, and (c) second heating.

Table 1. Theoretical and Experimental Molecular Weights Determined by GPC, Experimental Densities,[c] and Thermal Transitions of Monodendrons

monodendron	MW_t	M_n (GPC)	M_w/M_n (GPC)	M_n/MW_t	ρ_{20}[c] (g/cm^3)	thermal transitions (°C) and corresponding enthalpy changes (kcal/mol)[a] heating	cooling
4	1007.5	4303	1.01	4.27		k 33 (7.83) k 60 (24.68) k 67 (7.90) i k 66 (29.00) i[b]	i 40 (26.39) k
5	993.5	4169	1.02	4.20	1.02	k 47 (17.05)[b] −k 58 (1.31) k 70 (11.82) Φ_h145 (3.97) i k 43 (15.10)[b] Φ_h140 (3.71) i	i 136 (3.77) Φ_h 36 (15.43) k
7	3068.5	7306	1.02	2.38	1.02	k 47 (40.18) Φ_h 97 (2.28) Φ_h118 (0.65) i k −16 (19.58) Φ_h 98 (2.19) Φ_h 117 (0.52) i	i 107 (0.06) Φ_h 91 (2.55) Φ_h-23 (13.61) k
8	3096.6	7363	1.02	2.38	1.02	k 43 (36.63) Φ_h 92 (1.97) i k −16 (18.18) Φ_h 92 (1.74) i	i 85 (1.74) Φ_h −22 (11.55) k
12	3010.5	5277	1.10	1.75	1.01	k −1 (7.89) k 50 (22.74) Φ_h127 (3.05) i k −10 (14.75) Φ_h 127 (3.00) i	i 122 (3.25) Φ_h −15 (13.94) k
10	9251.7	10999	1.03	1.19	1.03	k −18 (16.61) −k 2 (4.70) T_g 46 Cub 178 (3.20) Cub 197 (3.00) i k −17 (10.25) T_g 47 Cub 179 (1.72) Cub 197 (2.36) i	i 188 (0.51) Cub 152 (1.77) Cub 136 (1.15) T_g 42 k −23 (35.25) k
11	9279.7	10894	1.02	1.17	1.03	k 1 (135.61) Cub 168 (1.35) i k −19 (41.09) Cub 167 (2.13) i	i 148 (0.78) Cub −18 (39.10) k

[a] Data from the first heating and cooling scans are on the first line, and data from the second heating are on the second line. [b] Sum of enthalpies from overlapped peaks. [c] Densities were measured at 20 °C.

Table 2. Structural Characterization of Supramolecular Dendrimers Self-Assembled from Selected Examples of Monodendrons

monodendron	T (°C)	d_{100} (Å)	d_{110} (Å)	d_{200} (Å)	d_{210} (Å)	d_{211} (Å)	$\langle d_{100}\rangle$[a] (Å)	a (Å)	R (Å)	S[f] (Å)	μ'	μ	ρ_{20}[j] (g/cm^3)
5	87	35.40		17.70			35.40	40.90[b]	20.40[d]	23.60		4.0[h]	1.02
7	70	41.70	23.72	20.45			41.23	47.61[b]	23.80[d]	27.49		2.0[h]	1.02
8	70	42.00	23.58	20.24			41.11	47.47[b]	23.74[d]	27.41		2.0[h]	1.02
12	60	42.40		19.60			40.80	47.11[b]	23.56[d]	27.20		2.0[h]	1.01
10	140			44.57	39.86	36.37		89.52[c]	24.53[e]		47.83[g]	6.0[i]	1.03

[a] $\langle d_{100}\rangle = (d_{100} + \sqrt{3}d_{110} + 2d_{200})/3$. [b] $a = 2\langle d_{100}\rangle/\sqrt{3}$. [c] $a = (\sqrt{2}d_{100} + \sqrt{4}d_{200} + \sqrt{5}d_{210} + \sqrt{6}d_{211} + \sqrt{8}d_{220})/5$ = lattice parameter. [d] $R = \langle d_{100}\rangle/\sqrt{3}$ = column radius. [e] $R = (0.548^c a)/2$ = spherical radius. [f] $S = 2R/\sqrt{3}$ = hexagon vertex. [g] $\mu' = (^c a^3\rho)/M$ = number of monodendrons per unit cell. [h] $\mu = (3\sqrt{3}N_A S^2 t\rho)/2M$ = number of monodendrons per cylinder stratum ($N_A = 6.022045 \times 10^{23}$ mol^{-1} (Avogadro's number), $t = 4.7$ Å = the average height of the column stratum, M = molecular weight of monodendron). [i] $\mu = \mu'/8$ = number of monodendrons per spherical dendrimer. [j] ρ_{20} = experimental density at 20 °C.

therefore, excluded. The construction of a column stratum from two hemidiscotic molecules of **8** and **12**, according to the XRD results summarized in Table 3, is shown in Figure 3.

Conclusions

The experiments described here present for the first time the shape analysis for a series of self-assembling monodendritic

Scheme 4. Self-Assembly of Monodendrons into Supramolecular Dendrimers

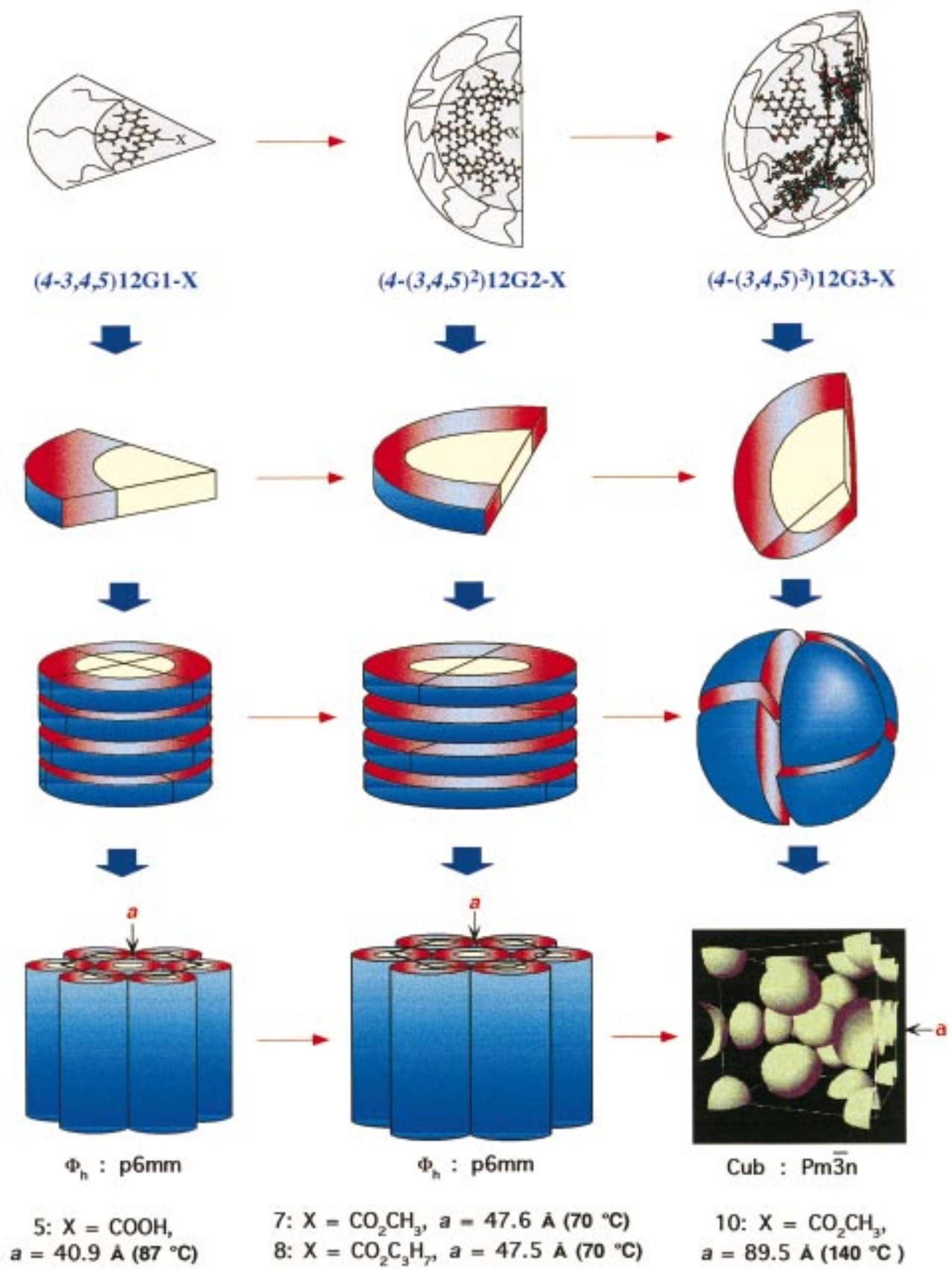

building blocks and of the corresponding supramolecular dendrimers as a function of generation number. The first- and second-generation monodendrons have shapes that are fragments of a disklike molecule, i.e., a quarter and a half of a disk, respectively. The third-generation monodendron is a sixth of a sphere. For this particular AB_3 system, the most dramatic

Scheme 5. Self-Assembly of **(*3,4,5*)^{4}12G4-COOH** (See Ref 7) and of **10** Monodendrons into Supramolecular Dendrimers

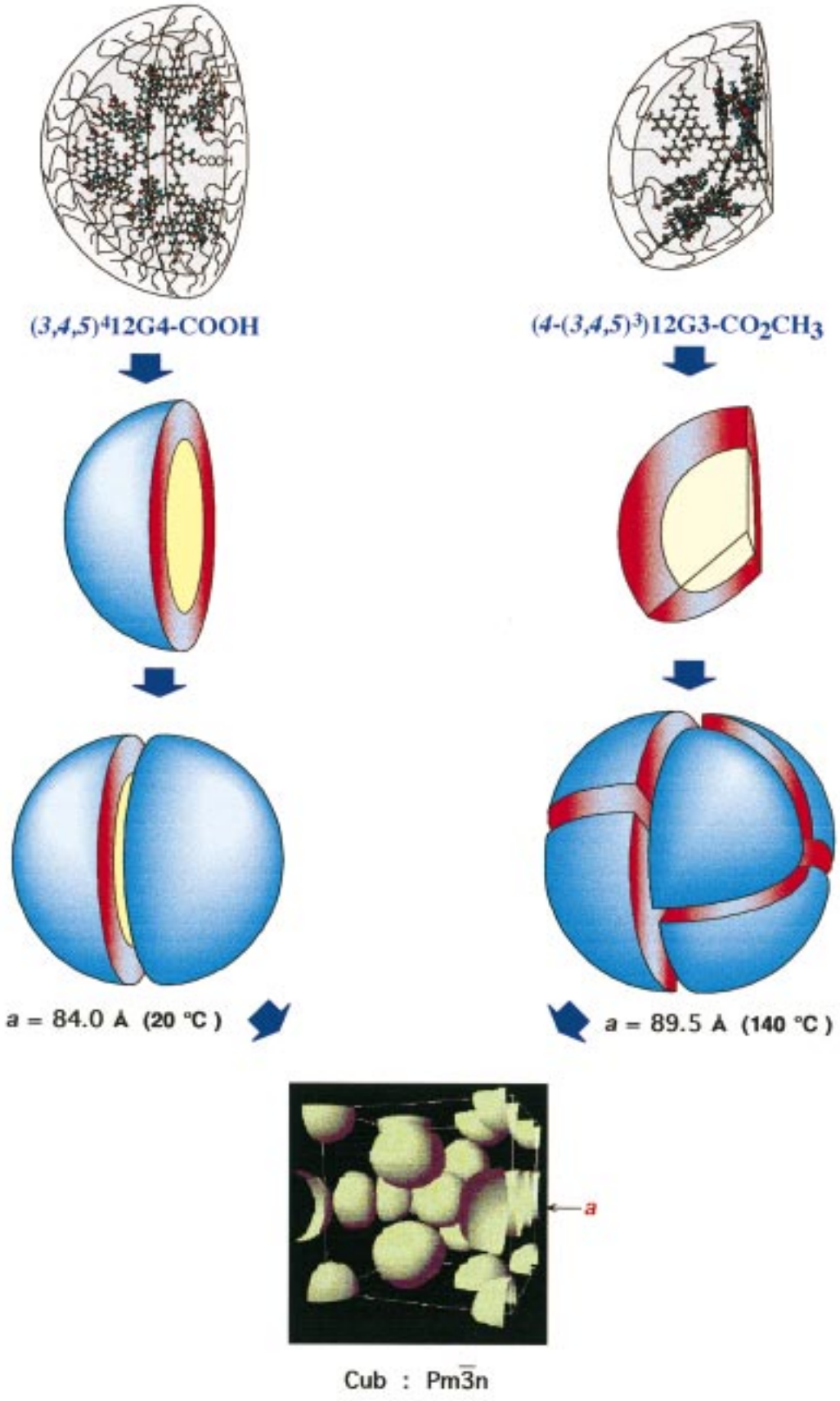

change in monodendron shape (i.e., from hemisphere to a sixth of a sphere) and in the resulting supramolecular dendrimer (i.e., from cylindrical to spherical) occurs at the transition from generation two to three. The generation number at which this shape change occurs should depend on monodendron architecture and functional group(s) in its core and on its periphery.

Table 3. Comparison of Alkyl Tail Shrinkage for **8** and **12** (See Figure 3 for Definition of R_{ext}, R_{core}, and R_{exp})

compound	no. of monodendrons per column stratum	t^a (Å)	R_{ext} (Å)	R^b_{core} (Å)	R_{exp} (Å)	shrinkage[c] (%)
8	1.0	2.58	28.4	12.6	23.7	29.8
	2.0	4.7	33.3	18.0	23.7	62.8
12	1.0	2.56	26.8	13.8	23.6	24.6
	2.0	4.7	31.6	19.2	23.6	64.5

[a] Height of column stratum, t required to accommodate an integer number of monodendrons in the stratum; $t = 4.7$ Å was taken from ref 16. [b] Aromatic core is elliptical, and, therefore, an average core radius is used. [c] Calculated % shrinkage $= [(R_{ext} - R_{exp})/(R_{ext} - R_{core})] \times 100$.

Previous publications have demonstrated only the irreversible dendrimer shape change from spherical to cylindrical induced by backbone multiplicity.[9,15]

Experimental Section

A. Materials. Methyl 3,4,5-trihydroxybenzoate (98%), 1-bromododecane (97%), methyl 4-hydroxybenzoate (99%), $LiAlH_4$ (95+%), $SOCl_2$ (99.5+%) (all from Aldrich), propyl 3,4,5-trihydroxybenzoate (98%), phloroglucinol anhydrous (98%) (from Lancaster), anhydrous K_2CO_3, DMF, THF, acetone, and EtOH (from Fisher, ACS reagent) were all used as received. CH_2Cl_2 (from Fisher, ACS reagent) was dried over CaH_2 and freshly distilled before use. THF and Et_2O (from Fisher, ACS reagent) were refluxed over sodium ketyl until the solution turned purple and then distilled before use.

B. Techniques. ^{1}H NMR (200 MHz) and ^{13}C NMR (50 MHz) spectra were recorded on a Varian Gemini 200 spectrometer at 20 °C with tetramethylsilane (TMS) as internal standard. The purity of products was determined by a combination of thin-layer chromatography (TLC) on silica gel plates (Kodak) with fluorescent indicator and high-pressure liquid chromatography (HPLC) using a Perkin-Elmer Series 10 high-pressure liquid chromatograph equipped with an LC-100 column oven, a Nelson Analytical 900 series integrator data station, and two Perkin-Elmer PL gel columns of 5×10^2 and 1×10^2 Å. THF was used as solvent at an oven temperature of 40 °C. Detection was by UV absorbance at 254 nm. Relative weight-average (M_w) and number-average (M_n) molecular weights were determined on the same instrument from a calibration plot constructed with polystyrene standards. Thermal transitons were measured on a Perkin-Elmer DSC-7 differential scanning calorimetry (DSC) equipped with a TADS data station. In all cases, the heating and cooling rates were 10 °C/min. First-order transition temperatures were reported as the maxima and minima of their endothermic and exothermic peaks. The transition temperatures (T_g) were read at the middle of the change in heat capacity. Indium and zinc were used as calibration standards. An Olympus BX-40 thermal optical polarized microscope (100× magnification) equipped with a Mettler FP 82 hot stage and a Mettler FP 80 central processor was used to verify thermal transitions and characterize the anisotropic textures. Small-angle X-ray diffractograms (SAXD) from powder samples were recorded with a quadrant detector at Station 8.2 of the Synchotron Radiation Source at Daresbury, U.K. Small- and wide-angle X-ray diffractograms from monodomain samples were recorded with an image plate area detector (MAR Research) using graphite-monochromatized Cu Kα radiation. In both cases, samples in glass capillaries were held in a custom-built temperature cell controlled to within ±0.1 °C. The beampath up to the beamstop was either evacuated or flushed with N_2. Densities (ρ_{20}) were determined by flotation in gradient columns at 20 °C. Molecular modeling was performed on a Silicon Graphic Indi computer with Macromodel Version 5.0 from Columbia University and CSC Chem3D from Cambridge Scientific Computing, Inc.

C. Synthesis. 2,6-Di-*tert*-butyl-4-methylpyridine (DTBMP). DTBMP was synthesized according to a literature procedure,[17] mp 32−34 °C (lit.[17] mp 33−36 °C). Methyl *p*-(*n*-dodecan-1-yloxy)benzoate **(2)**, *p*-(*n*-dodecan-1-yloxy)benzyl alcohol **(3)**, *p*-(*n*-dodecan-1-yloxy)-benzyl chloride, methyl 3,4,5-tris[*p*-(*n*-dodecan-1-yloxy)benzyloxy]-benzoate **(4)**, and 3,4,5-tris[*p*-(*n*-dodecan-1-yloxy)benzyloxy]benzoic acid **((*4*-*3,4,5*)12G1-COOH) (5)** were synthesized as was described previously.[14]

General Procedure for the Synthesis of (*4*-(*3,4,5*)^n)12Gn-CH_2OH. 3,4,5-Tris[*p*-(*n*-dodecan-1-yloxy)benzyloxy]benzyl Alcohol ((*4*-*3,4,5*)-12G1-CH_2OH) (6). Compound **6** was prepared by the reduction of **(*4*-*3,4,5*)12G1-CO_2CH_3 (4)** with $LiAlH_4$ using a modified literature procedure.[12] Into a three-neck round-bottom flask, equipped with a condensor, ice bath, N_2 inlet−outlet, and magnetic stirrer, containing a suspension of $LiAlH_4$ (2.07 g, 54.6 mmol) in dry THF (500 mL), was added **4** (50.0 g, 49.6 mmol) slowly under a flow of N_2. After the addition was complete, the suspension was stirred for 2 h at room temperature. The reduction was shown to be complete by TLC and ^{1}H NMR analyses. The reaction mixture was quenched by successive dropwise addition of 2.5 mL of H_2O, 2.5 mL of 15% NaOH, and 7.5 mL of H_2O. At this point, H_2 evolution ceased. The granular salts were filtered and washed with THF. The solvent was distilled on a rotary evaporator, and the remaining solid was recrystallized from acetone/CH_2Cl_2 (3:1, 650 mL) to yield 45.1 g (92.8%) of white crystals. Purity (HPLC), 99+%; TLC (hexane/ethyl acetate, 3:1): $R_f = 0.33$. ^{1}H NMR ($CDCl_3$, δ, ppm, TMS): 0.88 (t, 9H, CH_3, $J = 6.7$ Hz), 1.26 (overlapped m, 54H, $CH_3(CH_2)_9$), 1.78 (m, 6H, CH_2CH_2OAr), 3.88−3.99 (overlapped t, 6H, CH_2CH_2OAr), 4.57 (s, 2H, ArCH_2OH), 4.93 (s, 2H, ArCH_2OAr, 4 position), 5.01 (s, 4H, ArCH_2OAr, 3,5 positions), 6.65 (s, 2H, Ar*H ortho* to CH_2OH), 6.78 (d, 2H, Ar*H meta* to CH_2-OAr, 4 position, $J = 8.5$ Hz), 6.90 (d, 4H, Ar*H meta* to CH_2OAr, 3,5 positions, $J = 8.5$ Hz), 7.26 (overlapped d, 2H, Ar*H ortho* to CH_2-OAr, 4 position), 7.34 (d, 4H, Ar*H ortho* to CH_2OAr, 3,5 positions, $J = 8.1$ Hz). ^{13}C NMR ($CDCl_3$, δ, ppm, TMS): 14.1 (CH_3), 22.7 (CH_2-CH_3), 26.1−29.6 ($(CH_2)_8$), 31.9 ($CH_3CH_2CH_2$), 65.2 (ArCH_2OH), 68.1 (CH_2CH_2OAr, 3,4,5 positions), 71.2 (ArCH_2OAr, 3,5 positions), 74.9 (ArCH_2OAr, 4 position), 106.7 (Ar*C ortho* to CH_2OH), 114.2−114.5 (Ar*C meta* to CH_2OAr, 3,4,5 positions), 129.1−130.2 (Ar*C ortho* to CH_2OAr and Ar*C ipso* to CH_2OAr 3,4,5 positions), 136.7 (Ar*C ipso* to CH_2OH), 153.1 (Ar*C meta* to CH_2OH), 159.0 (Ar*C para* to CH_2-OAr, 3,4,5 positions). Anal. Calcd for $C_{64}H_{98}O_7$: C, 78.48; H, 10.09. Found: C, 78.67; H, 9.89.

General Procedure for the Synthesis of (*4*-(*3,4,5*)^n)12Gn-CH_2Cl. 3,4,5-Tris[*p*-(*n*-dodecan-1-yloxy)benzyloxy]benzyl Chloride ((*4*-*3,4,5*)12G1-CH_2Cl). (*4*-*3,4,5*)12G1-CH_2Cl was obtained by the chlorination of **(*4*-*3,4,5*)12G1-CH_2OH (6)** with $SOCl_2$. Into a 250-mL one-neck round-bottom flask, equipped with magnetic stirrer and addition funnel, were placed **6** (5.00 g, 5.11 mol), 2,6-di-*tert*-butyl-4-methylpyridine (**DTBMP**) (2.10 g, 10.2 mmol), CH_2Cl_2 (80 mL), and a mixture of $SOCl_2$ (0.372 mL, 5.11 mmol) and CH_2Cl_2 (5 mL) was added dropwise very slowly at room temperature. After the addition was complete, quantitative conversion was observed by ^{1}H NMR and GPC. The solvent was distilled on a rotary evaporator and the product was used immediately in the next step.

General Procedure for the Synthesis of (*4*-(*3,4,5*)^n)12Gn-CO_2CH_3. Methyl 3,4,5-Tris{3′,4′,5′-tris[*p*-(*n*-dodecan-1-yloxy)benzyloxy]-benzyloxy}benzoate ((*4*-(*3,4,5*)^2)12G2-CO_2CH_3) (7). **7** was obtained by the etherification of methyl 3,4,5-trihydroxybenzoate with **(*4*-*3,4,5*)-12G1-CH_2Cl**. In a 1000-mL three-neck round-bottom flask equipped with N_2 inlet−outlet and Teflon-coated magnetic stirrer, a mixture of K_2CO_3 (8.44 g, 61.0 mmol), DMF (200 mL), and THF (40 mL) was thoroughly degassed with N_2 for 1 h. Methyl gallate (1.25 g, 6.79 mmol) was added, and the mixture was heated to 70 °C. **(*4*-*3,4,5*)-12G1-CH_2Cl** (20.3 g, 20.3 mmol) was added. After 4 h, the reaction was found to be complete by TLC and ^{1}H NMR analyses. No side products were observed. The reaction mixture was poured into ice−water (1.5 L) and stirred for 1 h. The crude product was extracted with CH_2Cl_2 and its solution was dried over $MgSO_4$. The resulting white product (15.8 g, 76.0%) was purified by column chromatography (basic Al_2O_3; CH_2Cl_2) followed by recrystallization from acetone/CH_2-Cl_2 (1:3, 350 mL). Purity (HPLC), 99+%; TLC (hexane/ethyl acetate, 5:1): $R_f = 0.53$. ^{1}H NMR ($CDCl_3$, δ, ppm, TMS): 0.89 (t, 27H, CH_3, $J = 7.0$ Hz), 1.27 (overlapped m, 162H, $CH_3(CH_2)_9$), 1.75 (overlapped m, 18H, CH_2CH_2OAr), 3.84−3.91 (overlapped m, 21H, CH_2CH_2OAr, CO_2CH_3), 4.73−4.75 (overlapped s, 6H, ArCH_2OAr, 4-(3′,4′,5′) positions), 4.86 (s, 4H, ArCH_2OAr, 3,5-(4′) positions), 4.91 (s, 8H, ArCH_2-

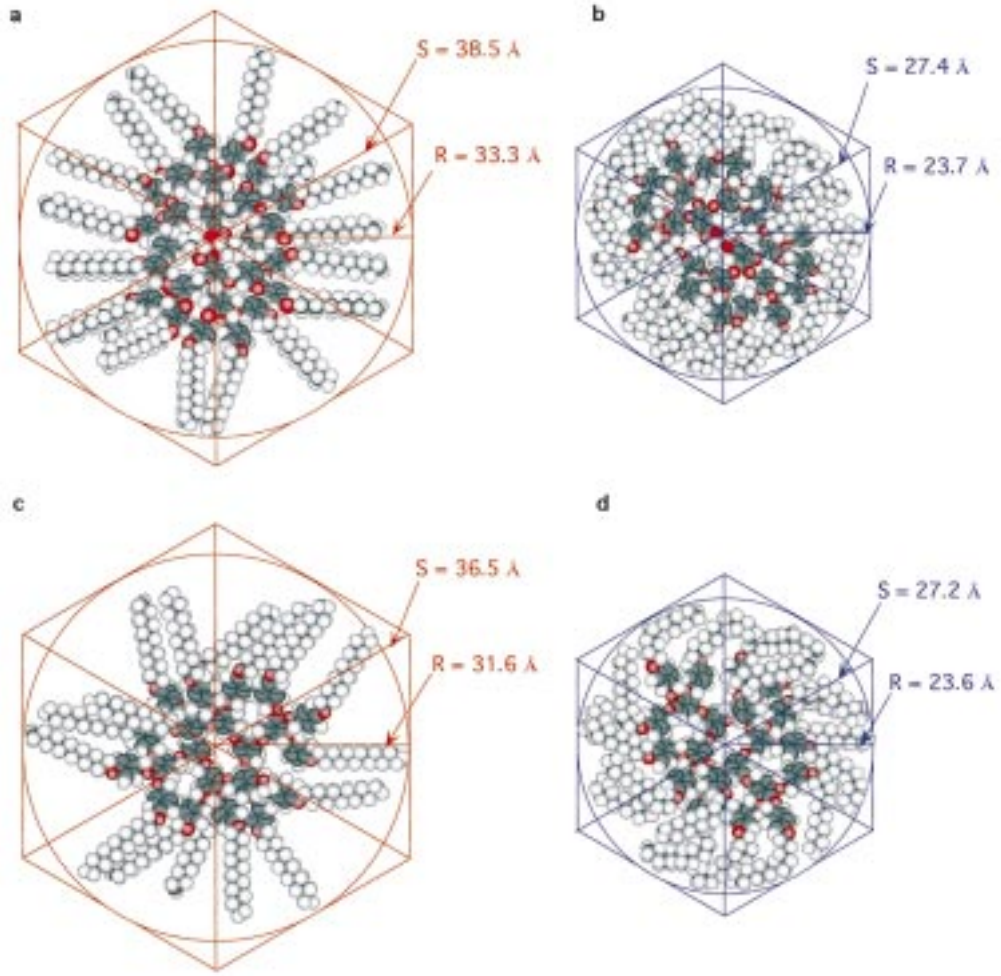

Figure 3. Schematic representation of the supramolecular column layer self-assembled from **8** with (a) alkyl tails extended and (b) alkyl tails melted, and of the supramolecular column layer self-assembled from **12** with (c) alkyl tails extended and (d) alkyl tails melted.

OAr, 3,5-(3′,5′) positions), 5.04−5.06 (overlapped s, 6H, ArCH_2OAr, 3,4,5 positions), 6.71−6.83 (overlapped m, 22H, Ar*H meta* to CH_2-OAr, 3,4,5-(3′,4′,5′) positions, Ar*H ortho* to CH_2OAr, 3,5 positions), 7.14−7.26 (overlapped m, 20H, Ar*H ortho* to CH_2OAr, 3,4,5-(3′,4′,5′) positions, Ar*H ortho* to CH_2OAr, 4 position), 7.41 (s, 2H, Ar*H ortho* to CO_2CH_3). ^{13}C NMR ($CDCl_3$, δ, ppm, TMS): 14.0 (CH_3), 22.6 (CH_2-CH_3), 26.1−29.6 ((CH_2)$_8$), 31.9 ($CH_3CH_2CH_2$), 68.0 (CH_2CH_2OAr, 3,4,5-(3′,4′,5′) positions), 71.0−71.7 (ArCH_2OAr, 3,4,5-(3′,5′) positions and 3,5 positions), 74.8−75.1 (ArCH_2OAr, 3,4,5-(4′) positions and 4 position), 107.3−107.8 (Ar*C ortho* to CH_2OAr, 3,4,5 positions), 110.0 (Ar*C ortho* to CO_2CH_3), 114.1−114.4 (Ar*C meta* to CH_2OAr, 3,4,5-(3′,4′,5′) positions), 129.1−130.0 (Ar*C ortho* to CH_2OAr and Ar*C ipso* to CH_2OAr, 3,4,5-(3′,4′,5′) positions), 132.1−132.8 (Ar*C para* to CH_2-OAr, 3,4,5 positions), 138.5 (Ar*C ipso* to CH_2OAr, 3,4,5 positions), 142.5 (Ar*C para* to CO_2CH_3), 152.6−153.2 (Ar*C meta* to CH_2OAr, 3,4,5 positions, Ar*C meta* to CO_2CH_3), 158.9 (Ar*C para* to CH_2OAr, 3,4,5-(3′,4′,5′) positions). Anal. Calcd for $C_{200}H_{296}O_{23}$: C, 78.28; H, 9.72. Found: C, 78.06; H, 9.56.

Propyl 3,4,5-Tris{3′,4′,5′-tris[*p*-(*n*-dodecan-1-yloxy)benzyloxy]-benzyloxy}benzoate ((*4*-(*3,4,5*)^2)12G2-$CO_2C_3H_7$) (8). Alkylation of propyl 3,4,5-trihydroxybenzoate (0.51 g, 2.4 mmol) with **(*4*-*3,4,5*)12G1-CH_2Cl** (7.14 g, 7.15 mmol) was performed in the presence of K_2CO_3 (2.97 g, 21.5 mmol) in a mixture of DMF (100 mL) and THF (10 mL) at 70 °C (4 h) by following the procedure described for **7** to yield 5.57 g (75.5%) of white solid after purification by column chromatography (basic Al_2O_3, CH_2Cl_2) and recrystallization from acetone/CH_2Cl_2 (1:3, 300 mL). Purity (HPLC), 99+%; TLC (hexane/ethyl acetate, 5:1): R_f = 0.48. ^{1}H NMR ($CDCl_3$, δ, ppm, TMS): 0.88 (t, 27H, CH_3, J = 6.8 Hz), 1.01 (t, 3H, $CO_2CH_2CH_2CH_3$, J = 7.6 Hz), 1.27 (overlapped m, 162H, $CH_3(CH_2)_9$), 1.76 (overlapped m, 20H, CH_2CH_2OAr, CO_2-$CH_2CH_2CH_3$), 3.80−3.93 (overlapped t, 18H, CH_2CH_2OAr), 4.26 (t, 2H, $CO_2CH_2CH_2CH_3$, J = 6.6 Hz), 4.73−4.75 (overlapped s, 6H, ArCH_2OAr, 4-(3′,4′,5′) positions), 4.85 (s, 4H, ArCH_2OAr, 3,5-(4′) positions), 4.91 (s, 8H, ArCH_2OAr, 3,5-(3′,5′) positions), 5.04−5.05 (overlapped s, 6H, ArCH_2OAr, 3,4,5 positions), 6.66−6.83 (overlapped m, 22H, Ar*H meta* to CH_2OAr, 3,4,5-(3′,4′,5′) positions, Ar*H ortho* to CH_2OAr, 3,5 positions), 7.14−7.26 (overlapped m, 20H, Ar*H ortho* to CH_2OAr, 3,4,5-(3′,4′,5′) positions, Ar*H ortho* to CH_2OAr, 4 position), 7.41 (s, 2H, Ar*H ortho* to $CO_2C_3H_7$). ^{13}C NMR ($CDCl_3$, δ, ppm, TMS): 14.1 (CH_3), 22.1 ($ArCO_2CH_2CH_2CH_3$), 22.6 (CH_2CH_3), 26.1−29.6 ((CH_2)$_8$), 31.9 ($CH_2CH_2CH_3$), 66.6 ($ArCO_2CH_2CH_2CH_3$), 68.0 (CH_2CH_2OAr, 3,4,5-(3′,4′,5′) positions), 71.0−71.7 (ArCH_2OAr, 3,4,5-(3′,5′) positions and 3,5 positions), 74.8−75.1 (ArCH_2OAr, 3,4,5-(4′) positions and 4 position), 107.3−107.8 (Ar*C ortho* to CH_2OAr, 3,4,5 positions), 110.0 (Ar*C ortho* to $CO_2C_3H_7$), 114.1−114.4 (Ar*C meta* to CH_2OAr, 3,4,5-(3′,4′,5′) positions), 129.1−130.0 (Ar*C ortho* to CH_2-OAr and Ar*C ipso* to CH_2OAr, 3,4,5-(3′,4′,5′) positions), 132.1−132.8 (Ar*C para* to CH_2OAr 3,4,5 positions), 138.5 (Ar*C ipso* to CH_2OAr, 3,4,5 positions), 142.5 (Ar*C para* to $CO_2C_3H_7$), 152.6−153.2 (Ar*C meta* to CH_2OAr, 3,4,5 positions, Ar*C meta* to $CO_2C_3H_7$), 158.9 (Ar*C para* to CH_2OAr, 3,4,5-(3′,4′,5′) positions). Anal. Calcd for $C_{202}H_{300}O_{23}$: C, 78.35; H, 9.77. Found: C, 78.31; H, 9.65.

3,4,5-Tris{3′,4′,5′-tris[*p*-(*n*-dodecan-1-yloxy)benzyloxy]benzyloxy}-benzyl Alcohol ((*4*-(*3,4,5*)^2)12G2-CH_2OH) (9). From **7** (11.0 g, 3.59 mmol) and $LiAlH_4$ (0.16 g, 4.2 mmol) in THF (200 mL) (2 h) was obtained 8.3 g (76%) of white solid after recrystallization from acetone/CH_2Cl_2 (1:4, 250 mL). Purity (HPLC), 99+%; TLC (hexane/ethyl acetate, 3:1): R_f = 0.63. ^{1}H NMR ($CDCl_3$, δ, ppm, TMS): 0.88 (t, 27H, CH_3, J = 6.8 Hz), 1.26 (overlapped m, 162H, $CH_3(CH_2)_9$), 1.75 (overlapped m, 18H, CH_2CH_2OAr), 3.81−3.92 (overlapped t, 18H,

CH_2CH_2OAr), 4.54 (s, 2H, $ArCH_2OH$), 4.76 (s, 6H, $ArCH_2OAr$, 4-(3′,4′,5′) positions), 4.85 (s, 4H, $ArCH_2OAr$, 3,5-(4′) positions), 4.90 (s, 8H, $ArCH_2OAr$, 3,5-(3′,5′) positions), 5.00 (s, 6H, $ArCH_2OAr$, 3,4,5 positions), 6.62−6.81 (s, 2H, Ar*H ortho* to CH_2OH), 6.65−6.81 (overlapped m, 26H, Ar*H meta* to CH_2OAr, 3,4,5-(3′,4′,5′) positions, Ar*H ortho* to CH_2OAr, 3,4,5 positions, Ar*H ortho* to CH_2OH), 7.15−7.25 (overlapped m, 18H, Ar*H ortho* to CH_2OAr, 3,4,5-(3′,4′,5′) positions). ^{13}C NMR ($CDCl_3$, δ, ppm, TMS): 14.1 (CH_3), 22.7 (CH_2CH_3), 22.7−29.7 ($(CH_2)_8$), 31.9 ($CH_3CH_2CH_2$), 65.0 (CH_2OH), 68.0 (CH_2CH_2OAr, 3,4,5-(3′,4′,5′) positions), 70.7−71.1 ($ArCH_2OAr$, 3,4,5-(3′,5′) positions and 3,5 positions), 74.8−75.3 ($ArCH_2OAr$, 3,4,5-(4′) positions and 4 position), 106.8−107.6 (Ar*C ortho* to CH_2OAr, 3,4,5 positions), 114.1−114.9 (Ar*C meta* to CH_2OAr, 3,4,5-(3′,4′,5′) positions), 129.1−130.0 (Ar*C ortho* to CH_2OAr and Ar*C ipso* to CH_2OAr, 3,4,5-(3′,4′,5′) positions), 132.7−133.4 (Ar*C para* to CH_2OAr, 3,4,5 positions), 137.6 (Ar*C ipso* to CH_2OH), 138.4 (Ar*C para* to CH_2OH), 152.9−153.2 (Ar*C meta* to CH_2OAr, 3,4,5 positions, Ar*C meta* to CH_2OH), 158.9 (Ar*C para* to CH_2OAr, 3,4,5-(3′,4′,5′) positions). Anal. Calcd for $C_{199}H_{296}O_{22}$: C, 78.61; H, 9.81. Found: C, 78.41; H, 9.89.

3,4,5-Tris{3′,4′,5′-tris[*p*-(*n*-dodecan-1-yloxy)benzyloxy]benzyloxy}-benzyl Chloride ((*4*-(*3,4,5*)^2)12G2-CH_2Cl). **(*4*-(*3,4,5*)^2)12G2-CH_2Cl** was synthesized by the procedure described for the synthesis of **(*4*-*3,4,5*)12G1-CH_2Cl**. This benzyl chloride was synthesized from **9** (2.00 g, 0.658 mmol), 2,6-di-*tert*-butyl-4-methylpyridine (DTBMP) (0.540 g, 2.63 mmol), and a mixture of $SOCl_2$ (0.078 g, 0.048 mmol) and CH_2Cl_2 (5 mL) in dry CH_2Cl_2 (40 mL) and was used without purification in the next step.

Methyl 3,4,5-Tris(3′,4′,5′-tris{3″,4″,5″-tris[*p*-(*n*-dodecan-1-yloxy)-benzyloxy]benzyloxy}benzyloxy)benzoate ((*4*-(*3,4,5*)^3)12G3- CO_2CH_3) (10). **10** was prepared according to the general procedure described for the synthesis of **7**. Starting from methyl 3,4,5-trihydroxybenzoate (0.12 g, 0.65 mmol), **(*4*-(*3,4,5*)^2)12G2-CH_2Cl** (5.98 g, 1.96 mmol), and K_2CO_3 (0.810 g, 5.87 mmol) in 130 mL of DMF and 12 mL of THF at 70 °C (5 h), a light yellow solid (4.78 g 79.3%) was obtained after purification by column chromatography (basic Al_2O_3; CH_2Cl_2) and recrystallization from acetone/CH_2Cl_2 (1:5, 250 mL). Purity (HPLC), 99+%; TLC (hexane/ethyl acetate, 20:1): $R_f = 0.65$. ^1H NMR ($CDCl_3$, δ, ppm, TMS): 0.91 (t, 81H, CH_3, J = 6.6 Hz), 1.29 (overlapped m, 486H, $CH_3(CH_2)_9$), 1.73 (overlapped m, 54H, CH_2CH_2OAr), 3.71−3.89 (overlapped m, 57H, CH_2CH_2OAr, CO_2CH_3), 4.45−5.13 (overlapped m, 78H, $ArCH_2OAr$), 6.45−7.25 (overlapped m, 132H, Ar*H meta* to CH_2OAr, Ar*H ortho* to CH_2OAr, 3,4,5-[3′,4′,5′−(3″,4″,5″)] positions, Ar*H ortho* to CH_2OAr, 3,4,5-(3′,4′,5′) positions, Ar*H ortho* to CH_2OAr, 3,4,5 positions), 7.50 (s, 2H, Ar*H ortho* to CO_2CH_3). ^{13}C NMR ($CDCl_3$, δ, ppm, TMS): 14.0 (CH_3), 22.7 (CH_2CH_3), 26.1−30.5 ($(CH_2)_8$), 31.9 ($CH_3CH_2CH_2$), 67.9 (CH_2CH_2OAr, 3,4,5-[3′,4′,5′-(3″,4″,5″)] positions), 70.8−71.6 ($ArCH_2OAr$, 3,4,5-[3′,4′,5′-(3″,5″)] positions, 3,4,5-(3′,5′) positions and 3,5 positions), 74.8−75.1 ($ArCH_2OAr$, 3,4,5-[3′,4′,5′-(4″)] positions, 3,4,5-(4′) positions and 4 position), 106.9−107.4 (Ar*C ortho* to CH_2OAr, 3,4,5-(3′,4′,5′) positions and 3,4,5 positions), 114.0−114.3 (Ar*C meta* to CH_2OAr, 3,4,5-[3′,4′,5′-(3″,4″,5″)] positions), 129.1−130.0 (Ar*C ortho* to CH_2OAr and Ar*C ipso* to CH_2OAr, 3,4,5-[3′,4′,5′-(3″,4″,5″)] positions), 132.3−132.8 (Ar*C para* to CH_2OAr, 3,4,5-(3′,4′,5′) positions and 3,4,5 positions), 138.5 (Ar*C ipso* to CH_2OAr, 3,4,5-(3′,4′,5′) and 3,4,5 positions), 153.2 (Ar*C meta* to CH_2OAr, 3,4,5-(3′,4′,5′) positions and 3,4,5 positions, Ar*C meta* to CO_2CH_3), 158.9 (Ar*C para* to CH_2OAr, 3,4,5-[3′,4′,5′-(3″,4″,5″)] positions). Anal. Calcd for $C_{605}H_{890}O_{68}$: C, 78.54; H, 9.70. Found: C, 78.59; H, 9.80.

Propyl 3,4,5-Tris(3′,4′,5′-tris{3″,4″,5″-tris[*p*-(*n*-dodecan-1-yloxy)-benzyloxy]benzyloxy}benzyloxy)benzoate ((*4*-(*3,4,5*)^3)12G3-$CO_2C_3H_7$) (11). From **(*4*-(*3,4,5*)^2)12G2-CH_2Cl** (3.50 g, 1.14 mmol), propyl 3,4,5-trihydroxybenzoate (0.081 g, 0.382 mmol), K_2CO_3 (0.480 g, 3.47 mmol), 60 mL of DMF, and 10 mL of THF at 70 °C (5 h), 2.68 g (75.7%) of a white solid was obtained after purification by column chromatography (basic Al_2O_3; CH_2Cl_2) and recrystallization from acetone/CH_2Cl_2 (1:5, 200 mL). Purity (HPLC), 99+%; TLC (hexane/ethyl acetate, 20:1): $R_f = 0.63$. ^1H NMR ($CDCl_3$, δ, ppm, TMS): 0.91 (t, 81H, CH_3, J = 6.6 Hz), 1.05 (t, 3H, $CO_2CH_2CH_2CH_3$, J = 7.4 Hz), 1.29 (overlapped m, 486H, $CH_3(CH_2)_9$), 1.73 (overlapped m, 56H, CH_2CH_2OAr, $CO_2CH_2CH_2CH_3$), 3.71−3.87 (overlapped m, 54H, CH_2CH_2OAr), 4.26 (t, 2H, $CO_2CH_2CH_2CH_3$, J = 6.6 Hz), 4.45−5.18 (overlapped m, 78H, $ArCH_2OAr$), 6.48−7.24 (overlapped m, 132H, Ar*H meta* to CH_2OAr, Ar*H ortho* to CH_2OAr, 3,4,5-[3′,4′,5′-(3″,4″,5″)] positions, Ar*H ortho* to CH_2OAr, 3,4,5-(3′,4′,5′) positions, Ar*H ortho* to CH_2OAr, 3,4,5 positions), 7.53 (s, 2H, Ar*H ortho* to CO_2CH_3). ^{13}C NMR ($CDCl_3$, δ, ppm, TMS): 14.0 (CH_3), 22.7 (CH_2CH_3), 26.1−30.1 ($(CH_2)_8$), 31.9 ($CH_3CH_2CH_2$), 67.9 (CH_2CH_2OAr, 3,4,5-[3′,4′,5′-(3″,4″,5″)] positions), 70.8−71.6 ($ArCH_2OAr$, 3,4,5-[3′,4′,5′-(3″,5″)] positions, 3,4,5-(3′,5′) positions and 3,5 positions), 74.7−75.3 ($ArCH_2OAr$, 3,4,5-[3′,4′,5′-(4″)] positions, 3,4,5-(4′) positions and 4 position), 106.9−107.3 (Ar*C ortho* to CH_2OAr, 3,4,5-(3′,4′,5′) positions and 3,4,5 positions), 114.0−114.2 (Ar*C meta* to CH_2OAr, 3,4,5-[3′,4′,5′-(3″,4″,5″)] positions), 129.1−129.8 (Ar*C ortho* to CH_2OAr and Ar*C ipso* to CH_2OAr, 3,4,5-[3′,4′,5′-(3″,4″,5″)] positions), 132.3−132.8 (Ar*C para* to CH_2OAr, 3,4,5-(3′,4′,5′) positions and 3,4,5 positions), 138.5 (Ar*C ipso* to CH_2OAr, 3,4,5-(3′,4′,5′) and 3,4,5 positions), 153.2 (Ar*C meta* to CH_2OAr, 3,4,5-(3′,4′,5′) positions and 3,4,5 positions, Ar*C meta* to $CO_2C_3H_7$), 158.7 (Ar*C para* to CH_2OAr, 3,4,5-[3′,4′,5′-(3″,4″,5″)] positions). Anal. Calcd for $C_{607}H_{894}O_{68}$: C, 78.57; H, 9.71. Found: C, 78.39; H, 9.71.

1,3,5-Tris[3,4,5-tris[*p*-(*n*-dodecan-1-yloxy)benzyloxy]benzyloxy]-benzene ((*4*-*3,4,5*-*1,3,5*)12G2-H) (12). Alkylation of phloroglucinol (0.215 g, 1.71 mmol) with **(*4*-*3,4,5*)12G1-CH_2Cl** (5.10 g, 5.12 mmol) (20 h) was carried out as described for **7**, yielding 2.89 g (56.3%) of light yellow solid after purification by column chromatography (basic Al_2O_3; ethyl acetate) and recrystallization from acetone/CH_2Cl_2 (1:3, 250 mL). Purity (HPLC), 99+%; TLC (hexane/ethyl acetate, 20:1): $R_f = 0.73$. ^1H NMR ($CDCl_3$, TMS, δ, ppm): 0.88 (t, 27H, CH_3, J = 6.3 Hz), 1.26 (overlapped m, 162H, $CH_3(CH_2)_9$), 1.77 (overlapped m, 18H, CH_2CH_2OAr), 3.91−3.97 (overlapped t, 18H, CH_2CH_2OAr), 4.89−4.92 (overlapped s, 12H, $ArCH_2OAr$, 1,3,5-(4′) positions, $ArCH_2OAr$, 1,3,5 positions), 5.01 (s, 12H, $ArCH_2OAr$, 1,3,5-(3′,5′) positions), 6.27 (s, 3H, Ar*H*, 2,4,6 positions), 6.73−6.77 (overlapped m, 12H, Ar*H meta* to CH_2OAr, 1,3,5-(4′) positions, Ar*H ortho* to CH_2OAr, 1,3,5 positions), 6.89 (d, 12H, Ar*H meta* to CH_2OAr, 1,3,5-(3′,5′) positions, J = 8.1 Hz), 7.29 (overlapped d, 6H, Ar*H ortho* to CH_2OAr, 1,3,5-(4′) positions, J = 6.2 Hz), 7.33 (overlapped d, 12H, Ar*H ortho* to CH_2OAr, 1,3,5-(3′,5′) positions, J = 8.1 Hz). ^{13}C NMR ($CDCl_3$, δ, ppm, TMS): 14.1 (CH_3), 22.7 (CH_2CH_3), 26.1−29.7 ($(CH_2)_8$), 31.9 ($CH_2CH_2CH_3$), 67.9 (CH_2CH_2OAr, 1,3,5-(3′,4′,5′) positions), 70.2−71.0 ($ArCH_2OAr$, 1,3,5-(3′,5′) positions and 1,3,5 positions), 74.8 ($ArCH_2OAr$, 1,3,5-(4′) positions), 94.9 (Ar*C ortho* to OCH_2Ar, 2,4,6 positions), 107.3 ($ArOCH_2$ *ortho* to CH_2OAr, 1,3,5 positions), 113.6−114.9 (Ar*C meta* to CH_2OAr, 1,3,5-(3′,4′,5′) positions), 128.6−130.1 (Ar*C ortho* to CH_2OAr and Ar*C ipso* to CH_2OAr, 1,3,5-(3′,4′,5′) positions), 132.1 (Ar*C para* to OCH_2Ar, 1,3,5 positions), 138.3 (Ar*C ipso* to CH_2OAr, 1,3,5 positions), 153.1 (Ar*C meta* to CH_2OAr, 1,3,5 positions), 158.9 (Ar*C para* to CH_2OAr, 1,3,5-(3′,4′,5′) positions), 160.6 (Ar*C ipso* to OCH_2Ar, 1,3,5 positions). Anal. Calcd for $C_{198}H_{294}O_{21}$: C, 79.00; H, 9.84. Found: C, 78.82; H, 9.79.

Acknowledgment. Financial support by the National Science Foundation (DMR-97-08581), the Engineering and Physical Science Research Council, UK, and the Synchrotron Radiation Source at Daresbury, UK, is gratefully acknowledged. We are also grateful to Professor S. Z. D. Cheng of University of Akron for determining the mass density data.

JA9819007